BIOCHEMISTRY
including biophysical chemistry & molecular biology
Article

Biochemistry **2010,** *49,* 5007–5015 5007
DOI: 10.1021/bi100280f

Binding of Fluorinated Phenylalanine α-Factor Analogues to Ste2p: Evidence for a Cation−π Binding Interaction between a Peptide Ligand and Its Cognate G Protein-Coupled Receptor[†]

Subramanyam Tantry,[‡] Fa-Xiang Ding,[‡] Mark Dumont,[§] Jeffrey M. Becker,[∥] and Fred Naider*[,‡,⊥]

[‡]*Department of Chemistry, College of Staten Island of the City University of New York, Staten Island, New York 10314,* [§]*University of Rochester School of Medicine and Dentistry, 601 Elmwood Avenue, Box 712, Rochester, New York 14642, and* [∥]*Department of Microbiology, University of Tennessee, Knoxville, Tennessee 37996* [⊥]*The Leonard and Esther Kurtz Term Professor at the College of Staten Island*

Received February 24, 2010; Revised Manuscript Received April 12, 2010

ABSTRACT: Ste2p, a G protein-coupled receptor (GPCR), binds α-factor, WHWLQLKPGQPMY, a tridecapeptide pheromone secreted by yeast cells. Upon α-factor binding, Ste2p undergoes conformational changes activating a signal transduction system through its associated heterotrimeric G protein leading to the arrest of cell growth in the G1 phase to prepare cells for mating. Previous studies have indicated that Tyr at position 13 of α-factor interacts with Arg58 on transmembrane one (TM1) of Ste2p. This observation prompted this investigation to determine whether a cation−π type of interaction occurred between these residues. Tyrosine at position 13 of α-factor was systematically substituted with analogous amino acids with varying cation−π binding energies using solid-phase peptide synthesis, and these analogues were modified by derivatization of their Lys^7 residue with the fluorescent group 7-nitrobenz-2-oxa-1,3-diazole (NBD) to serve as a useful probe for binding determination. Saturation binding of these peptides to Ste2p was assayed using whole yeast cells and a flow cytometer. In parallel the biological activities of the peptides were determined using a growth arrest assay. The data provide evidence for the presence of a cation−π interaction between Arg58 of Ste2p and Tyr^{13} of α-factor.

Understanding the molecular basis for the interaction of G protein-coupled receptors (GPCRs) with their cognate ligands has long been a thrust of scientific endeavor as these classes of seven-transmembrane (7-TM) receptors are pharmaceutical targets of over 40% of all approved drugs and are centrally involved in a broad spectrum of biological and pathological conditions (*1*). In the absence of X-ray crystal structures for all but the four GPCRs, rhodopsin, β_1-adrenergic, β_2-adrenergic, and adenosine receptors, drug discovery has relied upon ligand diversification and biological assays, receptor mutagenesis, and *in silico* tools such as computational and homology modeling to judge receptor−ligand interaction (*2*−*4*).

The α-factor receptor, Ste2p, is one of three GPCR's present in the yeast *Saccharomyces cerevisiae* (*5*). Despite the absence of sequence similarity between mammalian and yeast GPCRs, their mechanism of activation, signal transduction pathways, and 7-TM helical structures appear to be conserved. Evidence for this comes from the fact that Ste2p can activate the mammalian $G\alpha_{olf}$ subunit (*6*) and that heterologously expressed mammalian receptors such as the β_2-adrenergic receptor can activate the pheromone response pathway in yeast (*7*, *8*). Two charged cationic residues, Arg58 on TM1 and His94 on TM2, are predicted to reside at sites that are buried inside the hydrophobic membrane environment of Ste2p. A polar pair is highly conserved at these positions in the Ste2ps of various fungi, and molecular modeling experiments suggest that these residues project inward in the transmembrane region of these GPCRs (*9*).

An NMR study of the Ste2p fragment G31−T110 (TM1−TM2) in 1-palmitoyl-2-hydroxy-*sn*-glycero-3-[phospho-*rac*-(1-glycerol)] micelles reveals the presence of a highly flexible kink in the G56-VRS-G60 region of TM1 which divides TM1 into two helical sections and exposes the upper end of TM1 to the extracellular domain (*10*). Tyr^{13} of α-factor is believed to penetrate into the hydrophobic region of Ste2p and bind to the receptor near the extracellular face of TM1. The role of Tyr^{13} on the carboxy terminal of α-factor in binding to the receptor was previously investigated by our group through alanine scanning and photoaffinity labeling experiments (*11*, *12*). These studies showed that the presence of an aromatic residue at position 13 of α-factor is necessary for strong binding and optimal activity and that the contact point of position 13 of α-factor on the receptor involves residues Phe55−Arg58 on TM1. Recent studies using DOPA (3,4-dihydroxyphenylalanine) oxidative cross-linking with a $DOPA^{13}$-labeled α-factor analogue indicated that the contact point for this tyrosine surrogate was Cys59 on TM1 (*13*).

The cation−π interaction is a noncovalent interaction between a cation and the π-face of an aromatic ring. In biological contexts, it is usually an interaction between the cationic group of lysine or arginine and the π-face of the aromatic rings of phenylalanine, tyrosine, and tryptophan. The average strength of a cation−π interaction is about 3 kcal/mol, and it is now known to be an important contributor to the stabilization of protein secondary structures (reviewed in refs (*14*−*16*)). Cation−π interactions play prominent roles in the binding of neurotransmitters such as Ach,

[†]This work was supported by NIH Grants GM22087 (J.M.B. and F.N.) and GM059357 (M.D.).
*Corresponding author. Tel: 718-982-3896. Fax: 718-982-3910. E-mail: fred.naider@csi.cuny.edu.

Published on Web 04/26/2010

GABA, dopamine, NMDA, and adrenaline to their receptors (*17*). In the case of the well-studied nicotinic acetylcholine (nAchR) receptor, in which the binding pocket is made up of several tryptophan residues, progressive fluorination of Trp149 of the α-subunit resulted in a linear correlation between binding and the predicted cation−π binding energies of various analogues (*18*, *19*). Implementing similar strategies, the evaluation of the agonist binding site of the $GABA_c$ receptor, which has tyrosine at the aligning position, also revealed the presence of a cation−π type of interaction (*20*). Mutational studies of Tyr381 in the binding domain of the M1 muscarinic Ach receptor, along with evaluation of the affinity and signaling efficacy of three series of ligands, led to the conclusion that the Tyr381 benzene ring may form a cation−π interaction with acetylcholine ligand in the activated state but not in the ground state of this GPCR (*21*).

Given the existing knowledge of the importance of Tyr^{13} of α-factor in ligand binding and efficacy, the photoaffinity labeling investigations showing that Arg58 in Ste2p contacts Tyr^{13} of α-factor, the placement of Arg58 in the hydrophobic core of TM1, and the prominence of cation−π interactions in receptor−ligand recognition, we decided to explore the possibility that a cation−π interaction exists between α-factor and Ste2p. Tyr^{13} was substituted with various phenylalanine analogues and their agonist activities and equilibrium binding constants (K_d) were determined. Upon progressive fluorination of phenylalanine there was a linear increase in the K_d of the analogues. The fluorinated derivatives all retained some agonist activity, and wild-type α-factor efficiently competed with their binding to the receptor, indicating that the analogues interacted with the pheromone binding site of Ste2p. We conclude that there is evidence for a cation−π interaction between Tyr^{13} of α-factor and Arg58 of Ste2p.

EXPERIMENTAL PROCEDURES

Peptide Synthesis. All peptides were synthesized on an Applied Biosystems Model 433A automated peptide synthesizer using Fmoc/O^{t}Bu protection and HBTU as the coupling agent. Fastmoc 0.1 mmol chemistry designed by the manufacturer was employed for the chain assembly. The carboxyl-terminal Fmoc amino acids were coupled to a Wang resin (loading 0.4 mmol/g) on a 0.1 mmol scale using triple coupling, and the unreacted resin was capped with acetic anhydride. Subsequent chain assembly was carried out using a single coupling followed by acetic anhydride capping. After chain assembly, peptides were cleaved using trifluoroacetic acid (9.5 mL) and water (0.5 mL) with ethanedithiol (0.25 mL) as a scavenger. The reaction mixture was stirred for 2 h at room temperature and filtered. Evaporation of the reaction mixture at reduced pressure resulted in a gummy residue which was precipitated by addition of diethyl ether, and the crude peptide was isolated by centrifugation. The yield of the crude peptides ranged from 85% to 92%, and these were usually >80% homogeneous. After isolation, the crude Fmoc-α-factor analogues were purified using reverse-phase HPLC, and purification resulted in peptides with >90% homogeneity. The fluorescent group, 7-nitrobenz-2-oxa-1,3-diazole (NBD), was incorporated into the side chain of Lys^7 of α-factor using NBD-fluoride and the Fmoc-α-factor analogues following a previously described procedure (*22*), the Fmoc protection was removed *in situ*, and the crude reaction mixture was purified by reverse-phase preparative HPLC. The isolated yield of the Lys^7(NBD),Nle^{12},Tyr^{13}(substituted) α-factors was about 50% after purification, and all peptides used in binding analyses were >99% pure as judged by analytical HPLC and had the calculated molecular weights as determined by electrospray ionization mass spectrometry.

Saturation Binding Assays. Ligand stock solution was freshly prepared by dissolving a small amount of the [Lys^7-(NBD),Nle^{12}]α-factor analogue in 200 μL of methanol. Water was added to give a final volume of 400 μL of the methanol/water (1:1) stock. The UV absorbance at 470 nm of the ligand stock was then measured, and the concentration of the stock solution was calculated using a molar extinction coefficient (ε) of the peptide of 23000 M^{-1} cm^{-1} at 470 nm (*23*). Subsequent ligand dilutions were made using the concentration of this quantified stock solution as the starting peptide−ligand concentration.

Receptor binding assays were carried out using *S. cerevisiae* A3365 which contains a multicopy vector coding for expression of truncated Ste2p (Met_1−K_{304}) as reported previously (*23*), and *S. cerevisiae* A454 (*ste2*-Δ) which does not contain Ste2p was used as a negative control. Strain A454 contains a multicopy *URA3* vector (pMD228) with no insert in host strain A232 (*ste2*-Δ *ura3*$^-$ *leu2*$^-$ *bar1*). Both pMD228 and A232 are described earlier (*24*). Strain A3365 contains pMD1422, which encodes a truncated *STE2* allele in A232. pMD1422 was created by ligating a *Sac*I to *Sph*I fragment from pMD803 (*25*) containing a truncated *STE2* into plasmid pMD1383 also cut with *Sac*I and *Sph*I. pMD1383 was created by using site-directed mutagenesis to eliminate *Xba*I and *Hpa*I sites in pMD228 (see above) using oligonucleotides ON622 (AGATGCTTCGTTGACAAAGATAT) and ON623(TCCTATTCTCTGGAAAGTATAGGA).

Strain A3365 was cultured overnight at 30 °C in dropout SD-ura medium (*26*) until an OD_{600} of 0.8−1.2*A* was reached. A volume of culture corresponding to 1.5×10^6 cells (an OD_{600} of 1.0 corresponds to approximately 1.0×10^7 cells/mL) was transferred to microfuge tubes which were maintained on ice. The cultures were then diluted with ice-cold 20 mM sodium acetate/acetic acid buffer (pH 4.6) containing the desired concentration of ligand, and the final volume was adjusted to 400 μL. The methanol concentration in the final binding experiment never exceeded 3% by volume. The samples were incubated for 60 min (in the dark at 4 °C) and analyzed in triplicate over 30 min on an Accuri-c6 flow cytometer (Accuri cytometers, Inc., Ann Arbor, MI). The samples were excited at 488 nm (blue laser), and the fluorescence emitted at 530 ± 15 nm on the FL1-A channel was recorded. The fluorescence data were corrected for autofluorescence and were analyzed using Sigma Plot 8.0. The equilibrium binding constants K_d were obtained by fitting the data to a single site-specific binding equation, which included a nonspecific component *N*. The K_d values reported herein are the average of at least three independent experiments run on separate days using independently grown yeast cells.

Competition Binding Assay. Competition binding assays were performed on yeast strain A3365 expressing truncated Ste2p receptor (Δ304−431). The cells were streaked out from yeast master plates into 4 mL of SD-ura media and were grown at 30 °C overnight until they attained an OD_{600} of 1.0. NBD-labeled and unlabeled α-factor ligand solutions were prepared by dissolving a small amount of peptide in 500 μL of 1:1 MeOH:H_2O and were then quantified at 470 and 280 nm, respectively. After quantification, appropriate volumes of Lys^7(NBD),Nle^{12},Phe^{13}-(analogue) and unlabeled Lys^7,Nle^{12},Tyr^{13}(WT) α-factor were placed in 20 mM sodium acetate buffer (pH 4.6) in a microfuge tube. The solution was maintained at 4 °C, and the competition

binding assay was started by the addition of yeast culture corresponding to 1.5×10^6 cells/mL. The total volume of reaction mixture was 400 μL. The concentration of the NBD-labeled analogue used in the binding assays were 1.5 times their respective K_d and was 40 nM for Lys^7(NBD),Nle^{12},Phe^{13}(4-F), 60 nM for Lys^7(NBD),Nle^{12},Phe^{13}(3,4-F_2), and 300 nM for Lys^7(NBD), Nle^{12},Phe^{13}(2,3,4,5,6-F_5). The concentration of unlabeled α-factor, Lys^7,Nle^{12},Tyr^{13}(WT) used was 0, 0.3, 0.5, 1.0, 3.0, 5.0, 12, 50, 100, 250, 600, 1000, and 2000 nM. After incubation of samples for 60 min on an ice bath they were run on an Accuri-c6 flow cytometer in triplicate, and the mean fluorescence on the FL1A channel was measured. The mean fluorescence obtained was converted into percent bound and was plotted against the concentration of unlabeled Lys^7,Nle^{12},Tyr^{13}(WT) on a log scale.

Growth Arrest Halo Assay. Yeast strains A3365 (expressing truncated Ste2p receptor Δ304−431) and A454 (*ste2*-Δ) were grown to OD_{600} of 1.0 in 4 mL of SD-ura medium at 30 °C. The construction of these strains has been described earlier (*23*). A volume (1 mL) of culture corresponding to 6.0×10^6 cells was gently mixed with 1.0 mL of melted SD-ura medium containing 2% Difco agar and quickly spread over plates containing a bed of 2% SD-ura/agar. The plates were incubated for 2 h at 30 °C; then 6 μL portions of α-factor or α-factor analogues at various concentrations in 1:1 methanol:H_2O were spotted on top of the evenly spread yeast lawn. The plates were then incubated at 30 °C for 24−26 h until clearly demarcated halos were observed. Six microliters of 1:1 methanol:H_2O spotted as a control did not give rise to any halo formation. The assay was carried out in triplicate, and the reported values are the mean value of the halo diameters in millimeters. The halo sizes for the triplicate assays were within 1.0 mm for a given concentration. The concentrations of α-factor spotted for all of the analogues were 0, 1.56, 3.12, 6.25, 12.5, 25, and 50 μM. [Phe^{13}(2,3,4,5,6-F_5)]α-factor which did not give halos using the lower amount of the above concentrations was repeated using concentrations of 6.25, 12.5, 25, 50, 100, 200, and 400 μM. The halo diameters were plotted against the log of the concentration of α-factor. The data were fit to a linear regression curve using Sigma Plot 8.0. Relative activities were defined as the concentration of α-factor analogues giving rise to a halo diameter of 18 mm.

RESULTS

The K_d values for the binding of the various fluorophenylalanine analogues of α-factor to Ste2p were determined using a flow cytometer and the NBD-labeled pheromones. All analogues were synthesized by solid-state methods and were purified to high homogeneity using reversed-phase HPLC. All peptides were greater than 99% homogeneous as judged by HPLC and mass spectroscopy (data not shown).

Fluorescent Binding Analysis of Position 13 Analogues of α-Factor. In previous investigations we reported the use of the flow cytometric method for determining the binding affinity of [Lys^7(NBD),Nle^{12}]α-factor to various mutant forms of Ste2p (*23*). In these investigations 5−8-fold higher fluorescence values were obtained with truncated Ste2p as compared to full-length Ste2p because the truncated receptor is deficient in endocytosis resulting in higher receptor numbers on the cell membrane. However, both the truncated and full-length receptors exhibit nearly identical binding affinities for α-factor. We therefore decided to use the truncated receptor in the present investigation. Using this binding assay we found that the α-factor analogues with fluorinated phenylalanines at position 13 exhibited saturable binding to truncated Ste2p (A3365 strain) while the negative control experiments using a *ste2*-Δ deficient strain (A454) gave low background fluorescence which did not exhibit saturation (Figure 1). The results were highly reproducible, and the data could be fit to a single site binding equation which allowed us to account for a nonspecific binding component. Using this method we determined the binding affinities for fluorescently labeled wild-type sequence α-factor, [Lys^7(NBD), Phe^{13}]α-factor, [Lys^7(NBD),Phe^{13}(3-F)]α-factor, [Lys^7(NBD), Phe^{13}(4-F)]α-factor, [Lys^7(NBD),Phe^{13}(3,4-F_2)]α-factor, and [Lys^7(NBD),Phe^{13}(2,3,4,5,6-F_5)]α-factor (Table 1).

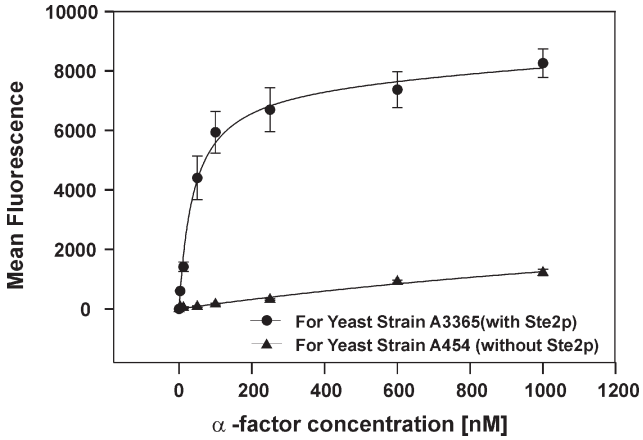

FIGURE 1: Representative saturation binding curve for [Lys^7(NBD), Nle^{12},Phe^{13}(3,4-F_2)]α-factor with yeast strains A3365 (with receptor) and A454 (without receptor).

Table 1: Effect of Substitution at Position 13 of α-Factor on Binding Affinity

entry	analogues of α-factor position 13 residue [Lys^7(NBD),X^{13}]α-factor	cation−π binding energy (kcal/mol)[b]	average K_d (nM)
1	tyrosine (wild type)	26.9	15.9 ± 3.5 (n = 3)
2	phenylalanine	27.1	20.4 ± 4.4 (n = 4)
3	3-fluorophenylalanine	22.0	31.4 ± 7.3 (n = 4)
4	4-fluorophenylalanine	22.0	26.2 ± 5.9 (n = 3)
5	3,4-difluorophenylalanine	17.4	38.1 ± 4.7 (n = 3)
6	pentafluorophenylalanine	3.9	177.3 ± 59.9 (n = 3)
7	alanine[a]	0	534.0 ± 137.3 (n = 3)
8	4-methylphenylalanine	28.6	53.2 ± 11.3 (n = 3)
9	4-methoxyphenylalanine	28.6	37.8 ± 20.9 (n = 5)

[a]The π-ring is absent; hence, cation−π binding energy is assumed to be zero. [b]References *27* and *28*.

Following approaches developed by Dougherty, Lester, and co-workers (*18*) we plotted the log of the K_d versus the previously published, calculated cation−π energies (*27*, *28*) for the fluorinated phenylalanine derivatives (Figure 2A). The data showed a linear correlation between log K_d and the cation−π binding energies. To further explore the possibility of a cation−π interaction, we synthesized three additional analogues: [Lys^7(NBD), Ala^{13}]α-factor, [Lys^7(NBD),Phe^{13}(4-CH_3)]α-factor, and [Lys^7-(NBD),Phe^{13}(4-OCH_3)]α-factor, compounds **7**, **8**, and **9**, respectively, in Table 1, and determined their binding constants (Table 1). These analogues either completely lacked cation−π interaction capabilities at position 13 (analogue **7**) or had slightly stronger predicted cation−π binding energies (analogues **8** and **9**) than α-factor. The [Lys^7(NBD),Ala^{13}]α-factor analogue showed extremely weak binding exhibiting at least a 30-fold decrease in affinity compared to [Lys^7(NBD)]α-factor, with significant

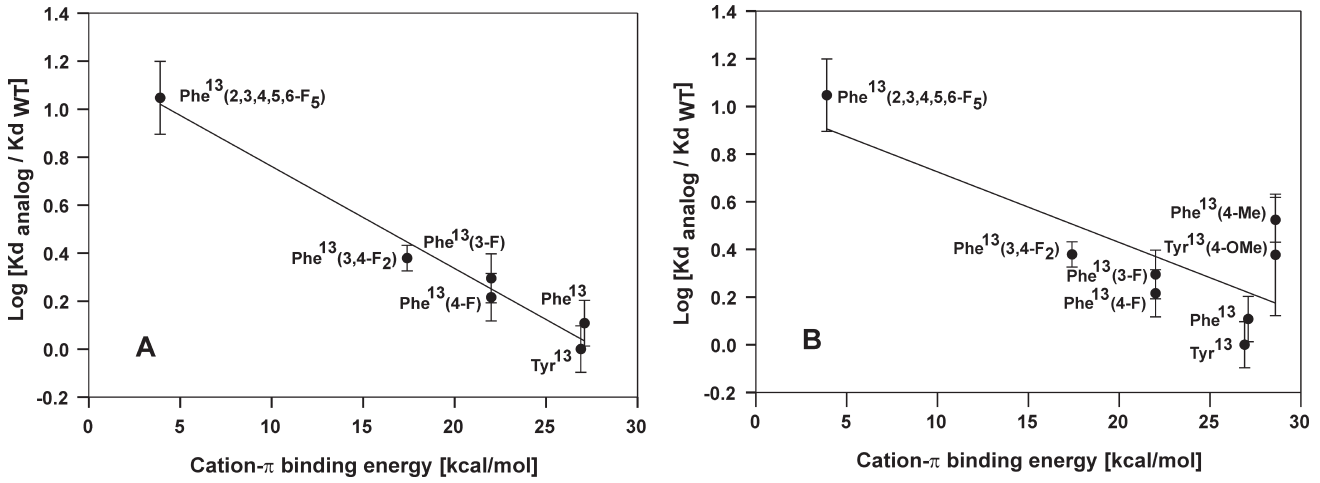

FIGURE 2: Plot of $\log[K_{d\,analogue}/K_{d\,WT}]$ vs cation$-\pi$ binding energy (A) for [Lys^7(NBD),Tyr^{13}]α-factor, [Lys^7(NBD),Phe^{13}]α-factor, [Lys^7(NBD),Phe^{13}(3-F)]α-factor, [Lys^7(NBD),Phe^{13}(4-F)]α-factor, [Lys^7(NBD),Phe^{13}(3,4-F$_2$)]α-factor, and [Lys^7(NBD),Phe^{13}(2,3,4,5,6-F$_5$)]-α-factor. The data were fitted into a straight line: $y = 1.186 - 0.0425x$. (B) Plot involving all position 13 analogues synthesized except [Lys^7(NBD),Ala^{13}]α-factor. The data were fitted into a straight line: $y = 1.021 - 0.0296x$. The K_d values were determined using saturation binding curves for the fluorescent analogues measured with the fluorescent activated flow cytometer as described in Experimental Procedures.

variability in the results. The [Lys^7(NBD),Phe^{13}(4-CH$_3$)]α-factor showed a decrease in affinity of approximately 3-fold compared to normal α-factor whereas the [Lys^7(NBD),Phe^{13}(4-OCH$_3$)]-α-factor had an affinity quite similar to the difluorophenylalanine analogues accompanied by a large deviation between individual assays. Inclusion of the latter two compounds in the log K_d versus cation$-\pi$ binding energy resulted in considerable scattering of the data and a weaker correlation between K_d and binding energy (Figure 2B).

Competition Binding Assay. It was important to ascertain whether the position 13 analogues bound to Ste2p at the same site as normal α-factor. We investigated this by determining whether normal unlabeled α-factor could compete with the fluorescently labeled fluorophenylalanine α-factors for binding to the receptor. Fluorescence binding analyses for three labeled α-factor analogues ([Lys^7(NBD),Phe^{13}(4-F)]α-factor, [Lys^7(NBD),Phe^{13}-(3,4-F$_2$)]α-factor, and [Lys^7(NBD),Phe^{13}(2,3,4,5,6-F$_5$)]α-factor) were conducted in the presence of increasing concentrations of unlabeled α-factor. Measurements were made using a concentration of the NBD-labeled α-factor analogue that was 1.5 times the K_d of the labeled ligand so that a strong fluorescence was initially measured but the receptor was not saturated by the analogue. The cells were incubated for 60 min on ice and run on an Accuri-c6 flow cytometer. The presence of unlabeled α-factor caused a sharp decrease in the fluorescence of the NBD-fluorophenylalanine α-factor analogues (Figure 3). While greater than 97% of the fluorescence from bound [Lys^7(NBD),Phe^{13}(4-F)]α-factor and [Lys^7(NBD),Phe^{13}(3,4-F$_2$)]α-factor could be competed out with unlabeled α-factor, only 83% of the fluorescence from bound [Lys^7(NBD),Phe^{13}(2,3,4,5,6-F$_5$)]α-factor was removed by this wild-type pheromone (Figure 3). The amount of unlabeled α-factor required to compete 50% of the bound labeled ligand is 30 nM for [Lys^7(NBD),Phe^{13}(4-F)]α-factor, 32 nM for [Lys^7-(NBD),Phe^{13}(3,4-F$_2$)]α-factor, and 10.5 nM in the case of [Lys^7-(NBD),Phe^{13}(2,3,4,5,6-F$_5$)]α-factor.

Biological Activities of the Position 13 Analogues of α-Factor: Growth Arrest Halo Assay. The biological activities of the position 13 α-factor analogues were determined using a halo assay of growth arrest in response to ligand. Increasing concentrations of α-factor or the various fluorophenylalanine

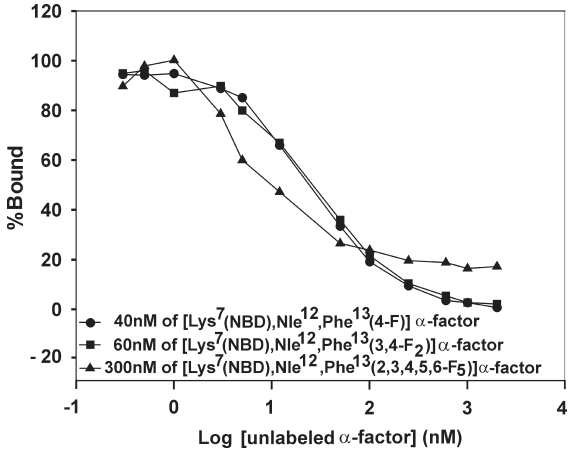

FIGURE 3: Competition between [Lys^7,Nle^{12},Tyr^{13}]α-factor (WT) and fluorescently labeled fluorophenylalanine analogues for binding to Ste2p. Plot of percentage of mean fluorescence bound vs log of α-factor concentration (nM).

analogues resulted in increased diameters for growth arrest on lawns of cultured *S. cerevisiae* strain A3365 expressing C-terminally truncated Ste2p (Figure 4B−D). No halo formation was observed with the *ste2*-Δ strain A454 (Figure 4A). All of the unlabeled fluorophenylalanine α-factor analogues except for [Lys^7,Phe^{13}(2,3,4,5,6-F$_5$)]α-factor gave sharply defined halos using ligand concentrations ranging from 1.56 to 50 μM. When assays with the pentafluorophenylalanine α-factor, which did not form a halo until 12.5 μM, were repeated with higher concentrations of ligand (12.5−400 μM), the resulting halos were comparable with those observed at lower concentrations of the other α-factor analogues (Figure 4B−D).

The halo size from the growth arrest assay was plotted versus log of the concentration of the pheromone (Figure 5). All analogues showed a linear correlation between the halo diameter and the log of concentration of the pheromone over the range of concentrations that were examined. These plots were then used to determine the analogue concentration required to give a halo diameter of 18 mm. The results showed that the [Lys^7,Tyr^{13}(*O*Me)]α-factor was the most potent agonist inducing an 18 mm halo at 1.66 μM concentration. It should be noted that the slope of the plot for this latter pheromone

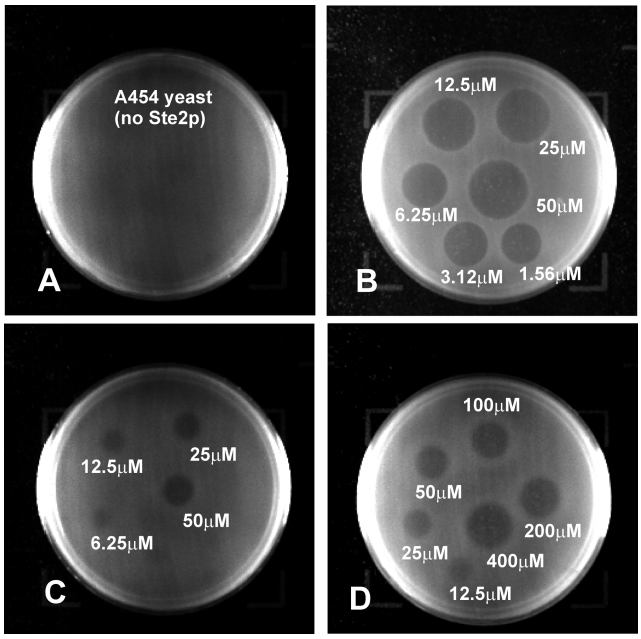

FIGURE 4: Growth arrest halo assay studied at different pheromone concentrations. (A) [Lys^7,Phe^{13}(3,4-F$_2$)]α-factor with yeast strain A454 and ligand concentration ranging from 1.56 to 50 μM. (B) [Lys^7,Phe^{13}(3,4-F$_2$)]α-factor with yeast strain A3365 and ligand concentration ranging from 1.56 to 50 μM. (C) [Lys^7,Phe^{13}(2,3,4,5,6-F$_5$)]α-factor with strain A3365 and ligand concentration ranging from 1.56 to 50 μM. (D) [Lys^7,Phe^{13}(2,3,4,5,6-F$_5$)]α-factor with strain A3365 and ligand concentration ranging from 12.5 to 400 μM.

differed from that of all of the other analogues. This likely reflects differences in the diffusion of this compound in the agar. The wild-type, mono-, di-, and pentafluoro analogues gave activities of 5.0, 5.4, 11.7, and 655.6 μM, respectively, using this assay. Thus although all analogues are agonists, the pentafluorophenylalanine^{13} analogue is about 130-fold less active than α-factor.

Four fluorescently labeled α-factor analogues ([Lys^7(NBD),Tyr^{13}]α-factor(WT), [Lys^7(NBD),Phe^{13}(4-F)]α-factor, [Lys^7(NBD),-Phe^{13}(3,4-F$_2$)]α-factor, and [Lys^7(NBD),Phe^{13}(2,3,4,5,6-F$_5$)]-α-factor) were also studied to determine whether the fluorescent Lys^7(NBD) analogues used in the binding study were agonists (Figure 5C). The overall halo diameters induced by NBD analogues were smaller compared to those of the unlabeled analogues. Since the overall diameters of the halos were smaller, the concentrations of NBD-labeled α-factor required to cause a 16 mm halo, rather than a 18 mm halo, were measured. Lys^7-(NBD)-labeled WT α-factor at 7.8 μM produced a 16 mm halo, whereas the labeled mono- and difluoro analogues produced a similar halo diameter at 25.6 and 66.8 μM, respectively. The activity of [Lys^7(NBD),Phe^{13}(2,3,4,5,6-F$_5$)]α-factor could not be measured by this method as the ligand started precipitating at concentrations above 25 μM where this α-factor analogue resulted in a halo which had a diameter of only 7 mm.

DISCUSSION

Earlier studies carried out by our group employing photoaffinity labeling with [benzoylphenylalanine^{13}]α-factor and oxidative cross-linking experiments involving DOPA^{13} α-factor suggested

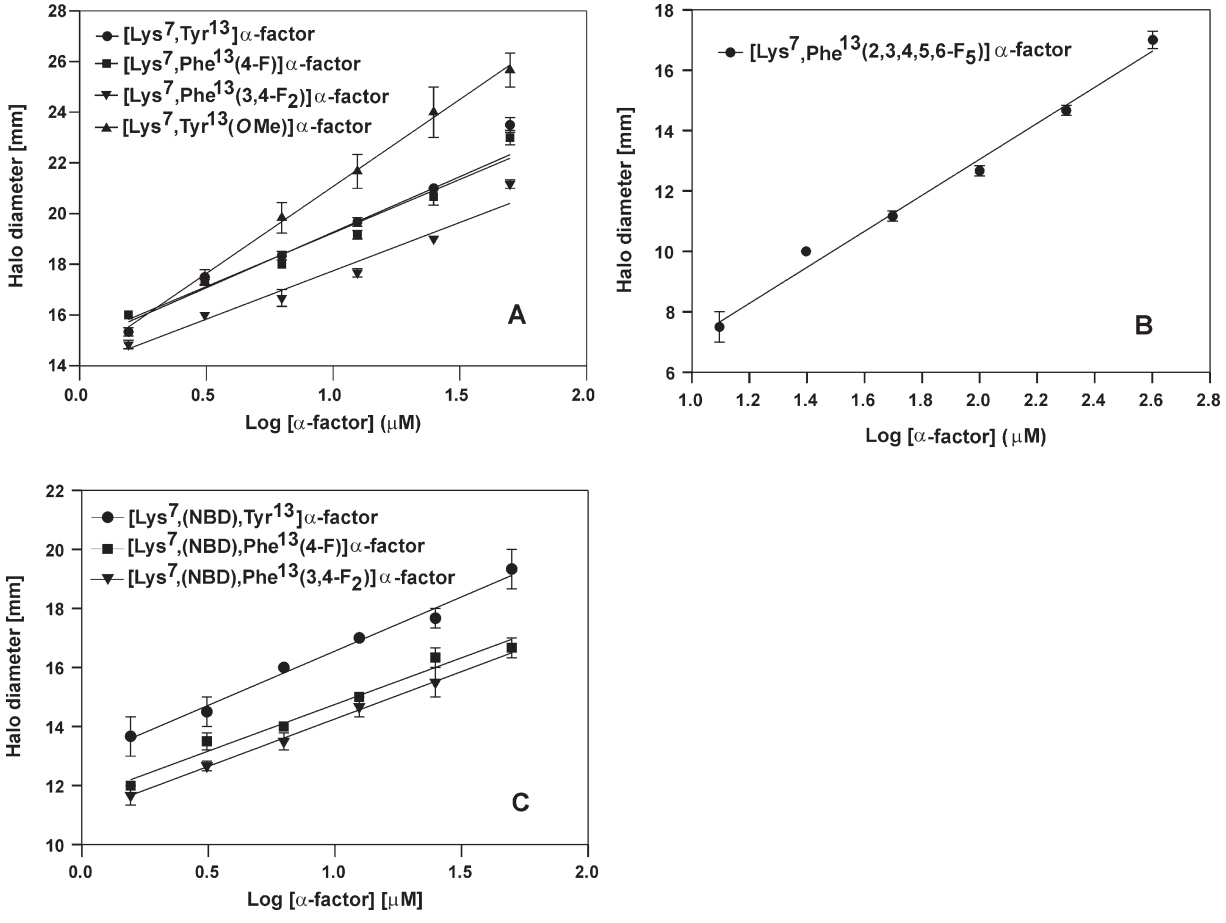

FIGURE 5: Plot of halo diameter vs log of pheromone concentration. (A) [Lys^7,Tyr^{13}]α-factor (WT), [Lys^7,Phe^{13}(4-F)]α-factor, [Lys^7,Phe^{13}-(3,4-F$_2$)]α-factor, and [Lys^7,Tyr^{13}(*O*Me)]α-factor. (B) [Lys^7,Phe^{13}(2,3,4,5,6-F$_5$)]α-factor. (C) [Lys^7(NBD),Tyr^{13}]α-factor, [Lys^7(NBD),Phe^{13}-(4-F)]α-factor, and [Lys^7(NBD),Phe^{13}(3,4-F$_2$)]α-factor analogues.

that the Tyr^{13} position of α-factor interacts with the TM1 segment of Ste2p at residues R58 and Cys59, respectively (*12*, *13*), and the presence of an aromatic ring at position 13 of α-factor was found to be necessary for efficient binding (*11*, *29*). Arg58 on TM1 and His94 on TM2 in Ste2p are believed to be in the hydrophobic core of the membrane. Other members of the fungal pheromone GPCR subfamily conserve polar residues at similar positions (*9*). The conservation of positively charged residues in the first and second TM domains of these fungal GPCRs and the critical nature of Tyr^{13} of α-factor and of other fungal α-factors suggested to us that ligand recognition by Ste2p might involve a cation−π type of interaction.

Fluorine substitution has been utilized as an important tool to track cation−π interactions as fluorine is sterically similar to hydrogen but due to its extremely high electronegativity has a remarkable effect on the electronic structure of an aromatic ring. Progressive fluorination of the aromatic ring decreases the π-electron density and thereby decreases the ability of the π-face to interact with cations. Previously, we studied [Phe^{13}]α-factor, [Phe^{13}(3-F)]α-factor, and [Phe^{13}(4-F)]α-factor using a radioactive binding competition assay and found that these analogues competed strongly with α-factor binding and were good agonists (*29*). In the present investigation, using a direct fluorescence saturation binding assay and multiple fluorinated peptides we studied α-factor analogues with varying predicted cation−π binding energies and revealed that there is significant influence of the cation−π binding energies of the phenylalanine ring on the equilibrium binding constant K_d of the receptor. Phenylalanine has a similar cation−π binding energy as that of tyrosine (*27*) (Table 1), and ideally phenylalanine replacement should not adversely affect the binding affinity. In our studies, the K_d obtained for [Phe^{13}]α-factor is similar to that of native [Tyr^{13}]α-factor, which appears to validate this contention.

Phe(3-F) (entry **3**, Table 1) and Phe(4-F) (entry **4**, Table 1) have similar calculated cation−π binding energies, and α-factor analogues with these substitutions were found to have similar K_d values in our binding studies. This indicates that the position of the fluorine atom does not have a significant effect on the binding affinity, and the trend that we begin to see is mainly due to the decrease in cation−π binding energy. Progressive fluorination of the phenylalanine ring resulted in an increase in K_d, and the data fit well onto a linear correlation plot (Figure 2A). Phe(2,3,4,5,6-F_5) has the lowest cation−π binding energy among the fluorinated α-factor derivatives that were studied, and this analogue exhibited approximately a 10-fold decrease in binding affinity compared to α-factor. The associated decrease in binding affinity due to fluorination is not of the magnitude that was reported for ligand-gated channels where up to a 2 log change in binding constants was observed. This suggests that the associated cation−π contribution to the α-factor−Ste2p binding may be weaker than the contribution to the ligand interactions in ion channels. In fact, we have recently found that position 13 of α-factor also interacts with Cys59 of Ste2p (*13*) so that contributions of H-bonding between the hydroxyl group of Tyr^{13} to Cys59 and a cation−π interaction between Tyr^{13} and Arg58 both contribute to the binding of α-factor to Ste2p.

An additional way to test for the cation−π interaction would be to carry out a similar binding analysis on *ste2* mutants where Arg58 is replaced by other residues. We have generated three such mutants (R58A, R58D, and R58E). All of these are seriously deficient in binding, with K_d's for α-factor from 10- to 50-fold higher. As shown in the present study the fluorescent fluorinated α-factor analogues had K_d's for the wild-type Ste2p ranging from 26.2 to 177.3 nM (Table 1). To determine the latter value, we needed to use 4 μM peptide, saturation was barely achieved, and the nonspecific fluorescence was quite high. Since the Ste2p containing the substitution R58A binds α-factor with nearly 10-fold lower affinity, saturation binding experiments would require very high concentrations of [Lys^7(NBD),Phe^{13}-(2,3,4,5,6-F_5)]α-factor (~40 μM). As stated above this peptide precipitates at 25 μM, and the experiment, therefore, could not be done. However, the marked decrease in affinity noted with the three *ste2* mutants that we generated supports our conclusion that the Arg58 side chain contributes to the binding energy and would be consistent with the cation−π interaction.

The use of NBD derivatives of α-factor might lead to a change in the interaction of position 13 of the pheromone and its receptor. However, all of the analogues that we tested were agonists, indicating productive binding to the receptor, and the potencies of the fluorinated α-factor analogues were within a factor of 3−4 of that of α-factor with the exception of the pentafluorinated analogue. Although the trends in the binding affinities were not directly parallel to the trends in the agonist potencies, we have observed a similar lack of correlation in our previous study with α-factor analogues (*29*). Moreover, the weakest binding fluorinated analogue ([Phe^{13}(2,3,4,5,6-F_5)]-α-factor) was by far the weakest agonist. Finally, α-factor efficiently competed with the binding of the Lys^7(NBD) analogues to Ste2p. On the basis of these observations and previous studies on α-factor derivatized at the Lys^7 side chain (*30*−*33*) we conclude that the fluorescent labeling does not result in a significant perturbation of the interactions of the position 13 side chain and the receptor. Interestingly, two nonfluorinated analogues, [Phe^{13}(4-Me)]α-factor and [Phe^{13}(4-OMe)]α-factor, each showed a marked lack of correlation between the K_d values and cation−π binding energies (Figure 2B). This finding contrasts with the correlation observed with fluorinated phenylalanine analogues (Figure 2A) and indicates that while the insertion of fluorine in place of a hydrogen results in primarily an electronic effect on the benzene ring, other groups can have both electronic and steric effects on binding. These analogues have marginally higher cation−π binding energies as compared to phenylalanine and tyrosine (Table 1) and would be predicted to result in stronger binding. We observed a 3-fold decrease in the binding ability for [Phe^{13}(4-Me)]α-factor, and the difference reduces to 2-fold upon reintroduction of phenolic oxygen, which should be a good electron donor. It is possible that the effect of reintroduction of the donor oxygen atom is at least partially nullified by the steric bulk of the methoxy group. Despite the fact that it cannot participate in a cation−π interaction, the [Lys^7(NBD),Ala^{13}]-α-factor does bind weakly to Ste2p. Thus, it is evident that additional effects involving steric, electrostatic, and perhaps van der Waals forces may also play a role in α-factor−Ste2p recognition at position 13 of the pheromone.

Biological Implications. The results of this paper support the existence of a cation−π interaction between the carboxyl-terminal Tyr^{13} residue of the α-factor peptide and the Arg58 residue in the first transmembrane domain of Ste2p. This interaction contributes to the favorable energetics of binding of ligand to receptor, since removal of Tyr from the carboxyl terminus drastically reduces the peptide affinity and leads to an inactive pheromone (*34*). However, this interaction involving the C-terminal of α-factor is not, by itself, sufficient for receptor activation because N-terminally truncated analogues

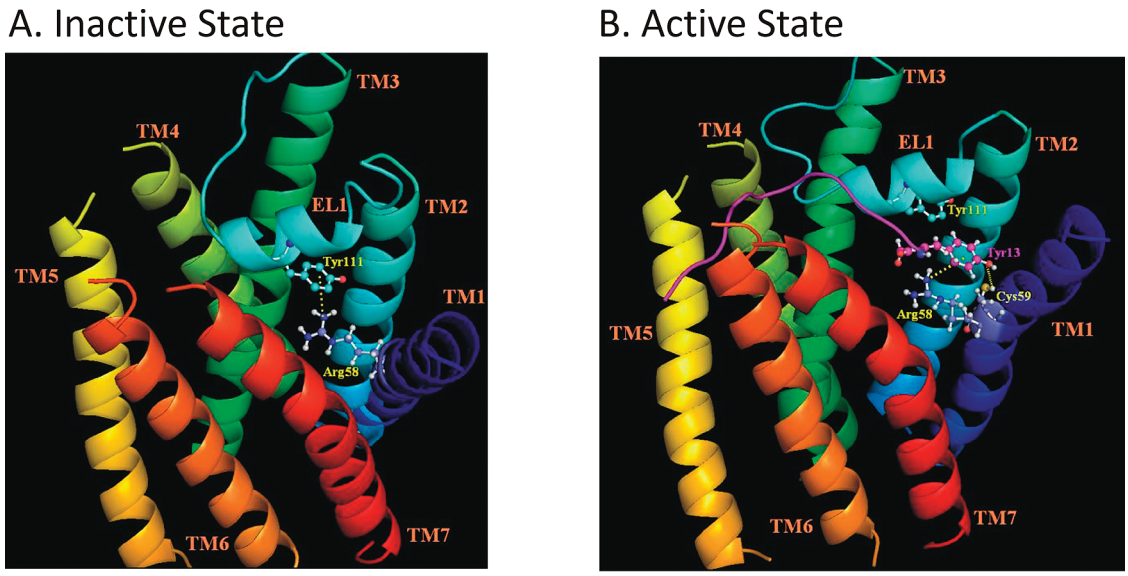

FIGURE 6: Model for change in EL1 loop receptor interactions in the presence and absence of α-factor. The transmembrane helices (TM) of Ste2p are shown in different colors and labeled. The structure of EL1 with a short 3_{10}-helix (^{106}YSSVTYALT^{114}) predicted by ref *46* is also shown. The α-factor in panel B is shown as a purple ribbon. Panel A: Cation−π interaction between the Arg58 guanidinium moiety in TM1 and the phenyl ring of Tyr111 (EL1) in the inactive state of Ste2p. Panel B: This interaction is disturbed upon α-factor binding and replaced by a similar cation−π interaction between Arg58 and Tyr^{13} of α-factor. The phenolic hydroxyl group of Tyr^{13} of α-factor is also suggested to form a hydrogen bond with the thiol group of Cys59. The interactions are shown as broken yellow lines.

of α-factor bind strongly to the receptor but do not lead to signal transduction (*34*).

Detection of the interaction of Arg58 of the receptor with Tyr^{13} of α-factor raises the question of how the positively charged Arg58 is accommodated when there is no ligand bound to receptor, since the existence of an isolated arginine side chain within the hydrophobic transmembrane region of Ste2p is expected to be energetically unfavorable. One possibility is that, in the absence of ligand, Arg58 participates in an intramolecular cation−π interaction with an aromatic residue elsewhere in the receptor. Each of the seven phenylalanine and two tryptophan residues within the predicted transmembrane regions of Ste2p can be mutated to nonaromatic residues without causing loss of function (*35*). Similarly, aromatic residues do not appear to be required at the positions of two of the three tyrosine residues in these regions. The remaining tyrosine, Tyr266, can only be mutated to Trp, Phe, or His (*35*, *36*). However, current models of Ste2p (*9*) place Tyr266 too far from Arg58 for any direct interaction.

This suggests that any aromatic side chain involved in an intramolecular cation−π interaction with Arg58 in the absence of ligand would reside in an extracellular tail or loop. The most likely site for the interacting side chains would be the first extracellular loop EL1, based on its expected proximity to Arg58 and on the following: (1) The results of cysteine scanning accessibility measurements on Ste2p indicate that burial of this loop in the transmembrane core of the receptor is involved in stabilizing the inactive state (*37*). (2) Mutation of Phe119, also in EL1, has been reported to lead to constitutive activity, as would be expected if EL1 is involved in stabilizing the inactive state (*38*). (3) Removal of residues 114−129 from EL1 of Ste2p yields a receptor that signals poorly but is constitutively active (Bhuiyan, Cohen, and Hauser unpublished results). (4) The substitution Tyr111C in EL1 of Ste2p results in a receptor that is incapable of signaling while retaining high-affinity α-factor binding, suggesting that Tyr111 is involved in the activation pathway.

Thus, we hypothesize that either Tyr111 or F119 in EL1 may interact with Arg58 in the ligand-free receptor via a π−cation interaction, stabilizing the ground state (see Figure 6 for a model of the Tyr111−Arg58 interaction in Ste2p). Upon ligand binding, the intramolecular interaction is replaced by the cation−π interaction with Tyr^{13} of α-factor, anchoring the carboxyl terminal of the ligand to the receptor and allowing the amino terminal of the pheromone to establish additional interactions that induce a conformational change that is propagated through other transmembrane domains, perhaps through the sequential actions of a series of "microswitches" (*39*), to sites interacting with the G protein. A role for EL1 in signal transduction by other GPCRs has been proposed based on studies of rhodopsin, the dopamine receptor, and the C5a receptor (*40*−*43*). In addition, recent solid-state and solution NMR studies have provided evidence for significant conformational changes in other extracellular loops of class A GPCRs (*44*, *45*).

CONCLUSION

We synthesized a series of position 13 α-factor analogues with varying predicted cation−π binding energies and applied a flow cytometry-based assay to investigate the binding of these peptide ligands to their cognate GPCR. The trends in K_d obtained by the fluorescence-based saturation binding experiments are well correlated with the predicted energies of a cation−π interaction for fluorinated phenylalanines at position 13 of α-factor. All analogues function as agonists and appear to bind to the α-factor pocket of Ste2p. The experimental results suggest that there is a cation−π interaction that facilitates binding of α-factor to Ste2p. However, electrostatic contributions associated with the phenolic oxygen of tyrosine and steric effects also appear to be involved in the interaction of position 13 and the receptor.

ACKNOWLEDGMENT

We thank Sara Connelly and Elizabeth Matthew for help in the binding and bioassays. We also thank Boris Arshava and

Leah Cohen for help with the preparation of the manuscript and George Umanah for preparation of Figure 6.

REFERENCES

1. Filmore, D. (2004) It's a GPCR World. *Mod. Drug Discovery 7*, 24–28.
2. Marshall, G. R. (2001) Peptide interactions with G-protein coupled receptors. *Biopolymers 60*, 246–277.
3. Kristiansen, K. (2004) Molecular mechanisms of ligand binding, signaling, and regulation within the superfamily of G-protein-coupled receptors: molecular modeling and mutagenesis approaches to receptor structure and function. *Pharmacol. Ther. 103*, 21–80.
4. Schyler, S., and Horuk, R. (2006) I want a new drug: G-protein-coupled receptors in drug development. *Drug Discovery Today 11*, 481–493.
5. Fredriksson, R., and Schioth, H. B. (2005) The repertoire of G-protein-coupled receptors in fully sequenced genomes. *Mol. Pharmacol. 67*, 1414–1425.
6. Crowe, M. L., Perry, B. N., and Connerton, I. F. (2000) Golf complements a GPA1 null mutation in *Saccharomyces cerevisiae* and functionally couples to the STE2 pheromone receptor. *J. Recept. Signal Transduction Res. 20*, 61–73.
7. King, K., Dohlman, H. G., Thorner, J., Caron, M. G., and Lefkowitz, R. J. (1990) Control of yeast mating signal transduction by a mammalian beta 2-adrenergic receptor and Gs alpha subunit. *Science (New York) 250*, 121–123.
8. Pausch, M. H. (1997) G-protein-coupled receptors in *Saccharomyces cerevisiae*: high-throughput screening assays for drug discovery. *Trends Biotechnol. 15*, 487–494.
9. Eilers, M., Hornak, V., Smith, S. O., and Konopka, J. B. (2005) Comparison of class A and D G protein-coupled receptors: common features in structure and activation. *Biochemistry 44*, 8959–8975.
10. Neumoin, A., Cohen, L. S., Arshava, B., Tantry, S., Becker, J. M., Zerbe, O., and Naider, F. (2009) Structure of a double transmembrane fragment of a G-protein-coupled receptor in micelles. *Biophys. J. 96*, 3187–3196.
11. Abel, M. G., Zhang, Y. L., Lu, H. F., Naider, F., and Becker, J. M. (1998) Structure-function analysis of the *Saccharomyces cerevisiae* tridecapeptide pheromone using alanine-scanned analogs. *J. Pept. Res. 52*, 95–106.
12. Son, C. D., Sargsyan, H., Naider, F., and Becker, J. M. (2004) Identification of ligand binding regions of the *Saccharomyces cerevisiae* alpha-factor pheromone receptor by photoaffinity cross-linking. *Biochemistry 43*, 13193–13203.
13. Umanah, G. K., Son, C., Ding, F., Naider, F., and Becker, J. M. (2009) Cross-linking of a DOPA-containing peptide ligand into its G protein-coupled receptor. *Biochemistry 48*, 2033–2044.
14. Ma, J. C., and Dougherty, D. A. (1997) The cation-pi interaction. *Chem. Rev. 97*, 1303–1324.
15. Gallivan, J. P., and Dougherty, D. A. (1999) Cation-pi interactions in structural biology. *Proc. Natl. Acad. Sci. U.S.A. 96*, 9459–9464.
16. Crowley, P. B., and Golovin, A. (2005) Cation-pi interactions in protein-protein interfaces. *Proteins 59*, 231–239.
17. Zacharias, N., and Dougherty, D. A. (2002) Cation-pi interactions in ligand recognition and catalysis. *Trends Pharmacol. Sci. 23*, 281–287.
18. Zhong, W., Gallivan, J. P., Zhang, Y., Li, L., Lester, H. A., and Dougherty, D. A. (1998) From ab initio quantum mechanics to molecular neurobiology: a cation-pi binding site in the nicotinic receptor. *Proc. Natl. Acad. Sci. U.S.A. 95*, 12088–12093.
19. Beene, D. L., Brandt, G. S., Zhong, W., Zacharias, N. M., Lester, H. A., and Dougherty, D. A. (2002) Cation-pi interactions in ligand recognition by serotonergic (5-HT3A) and nicotinic acetylcholine receptors: the anomalous binding properties of nicotine. *Biochemistry 41*, 10262–10269.
20. Lummis, S. C., Beene, D. L., Harrison, N. J., Lester, H. A., and Dougherty, D. A. (2005) A cation-pi binding interaction with a tyrosine in the binding site of the GABAC receptor. *Chem. Biol. 12*, 993–997.
21. Ward, S. D., Curtis, C. A., and Hulme, E. C. (1999) Alanine-scanning mutagenesis of transmembrane domain 6 of the M(1) muscarinic acetylcholine receptor suggests that Tyr381 plays key roles in receptor function. *Mol. Pharmacol. 56*, 1031–1041.
22. Ding, F. X., Lee, B. K., Hauser, M., Davenport, L., Becker, J. M., and Naider, F. (2001) Probing the binding domain of the *Saccharomyces cerevisiae* alpha-mating factor receptor with rluorescent ligands. *Biochemistry 40*, 1102–1108.
23. Bajaj, A., Celic, A., Ding, F. X., Naider, F., Becker, J. M., and Dumont, M. E. (2004) A fluorescent alpha-factor analogue exhibits multiple steps on binding to its G protein coupled receptor in yeast. *Biochemistry 43*, 13564–13578.
24. Leavitt, L. M., Macaluso, C. R., Kim, K. S., Martin, N. P., and Dumont, M. E. (1999) Dominant negative mutations in the alpha-factor receptor, a G protein-coupled receptor encoded by the STE2 gene of the yeast *Saccharomyces cerevisiae*. *Mol. Gen. Genet. 261*, 917–932.
25. Gehret, A. U., Bajaj, A., Naider, F., and Dumont, M. E. (2006) Oligomerization of the yeast alpha-factor receptor: implications for dominant negative effects of mutant receptors. *J. Biol. Chem. 281*, 20698–20714.
26. Rose, M., Winston, F., and Hieter, P. (1990) Methods in Yeast Genetics, Cold Spring Harbor Laboratory, Cold Spring Harbor, NY.
27. Mecozzi, S., West, A. P., Jr., and Dougherty, D. A. (1996) Cation-pi interactions in aromatics of biological and medicinal interest: electrostatic potential surfaces as a useful qualitative guide. *Proc. Natl. Acad. Sci. U.S.A. 93*, 10566–10571.
28. Raines, D. E., Gioia, F., Claycomb, R. J., and Stevens, R. J. (2004) The N-methyl-D-aspartate receptor inhibitory potencies of aromatic inhaled drugs of abuse: evidence for modulation by cation-pi interactions. *J. Pharmacol. Exp. Ther. 311*, 14–21.
29. Liu, S., Henry, L. K., Lee, B. K., Wang, S. H., Arshava, B., Becker, J. M., and Naider, F. (2000) Position 13 analogs of the tridecapeptide mating pheromone from *Saccharomyces cerevisiae*: design of an iodinatable ligand for receptor binding. *J. Pept. Res. 56*, 24–34.
30. Shenbagamurthi, P., Baffi, R., Khan, S. A., Lipke, P., Pousman, C., Becker, J. M., and Naider, F. (1983) Structure-activity relationships in the dodecapeptide alpha factor of *Saccharomyces cerevisiae*. *Biochemistry 22*, 1298–1304.
31. Raths, S. K., Naider, F., and Becker, J. M. (1988) Peptide analogues compete with the binding of alpha-factor to its receptor in *Saccharomyces cerevisiae*. *J. Biol. Chem. 263*, 17333–17341.
32. Naider, F., Yaron, A., Ewenson, A., Tallon, M., Xue, C. B., Srinivasan, J. V., Eriotou-Bargiota, E., and Becker, J. M. (1990) Synthetic probes for the alpha-factor receptor. *Biopolymers 29*, 237–245.
33. Naider, F., and Becker, J. M. (2004) The alpha-factor mating pheromone of *Saccharomyces cerevisiae*: a model for studying the interaction of peptide hormones and G protein-coupled receptors. *Peptides 25*, 1441–1463.
34. Eriotou-Bargiota, E., Xue, C. B., Naider, F., and Becker, J. M. (1992) Antagonistic and synergistic peptide analogues of the tridecapeptide mating pheromone of *Saccharomyces cerevisiae*. *Biochemistry 31*, 551–557.
35. Martin, N. P., Celic, A., and Dumont, M. E. (2002) Mutagenic mapping of helical structures in the transmembrane segments of the yeast alpha-factor receptor. *J. Mol. Biol. 317*, 765–788.
36. Lee, B. K., Lee, Y. H., Hauser, M., Son, C. D., Khare, S., Naider, F., and Becker, J. M. (2002) Tyr266 in the sixth transmembrane domain of the yeast alpha-factor receptor plays key roles in receptor activation and ligand specificity. *Biochemistry 41*, 13681–13689.
37. Hauser, M., Kauffman, S., Lee, B. K., Naider, F., and Becker, J. M. (2007) The first extracellular loop of the *Saccharomyces cerevisiae* G protein-coupled receptor Ste2p undergoes a conformational change upon ligand binding. *J. Biol. Chem. 282*, 10387–10397.
38. Parrish, W., Eilers, M., Ying, W., and Konopka, J. B. (2002) The cytoplasmic end of transmembrane domain 3 regulates the activity of the *Saccharomyces cerevisiae* G-protein-coupled alpha-factor receptor. *Genetics 160*, 429–443.
39. Nygaard, R., Frimurer, T. M., Holst, B., Rosenkilde, M. M., and Schwartz, T. W. (2009) Ligand binding and micro-switches in 7TM receptor structures. *Trends Pharmacol. Sci. 30*, 249–259.
40. Lawson, Z., and Wheatley, M. (2004) The third extracellular loop of G-protein-coupled receptors: more than just a linker between two important transmembrane helices. *Biochem. Soc. Trans. 32*, 1048–1050.
41. Shi, L., and Javitch, J. A. (2004) The second extracellular loop of the dopamine D2 receptor lines the binding-site crevice. *Proc. Natl. Acad. Sci. U.S.A. 101*, 440–445.
42. Klco, J. M., Wiegand, C. B., Narzinski, K., and Baranski, T. J. (2005) Essential role for the second extracellular loop in C5a receptor activation. *Nat. Struct. Mol. Biol. 12*, 320–326.
43. Klco, J. M., Nikiforovich, G. V., and Baranski, T. J. (2006) Genetic analysis of the first and third extracellular loops of the C5a receptor reveals an essential WXFG motif in the first loop. *J. Biol. Chem. 281*, 12010–12019.
44. Ahuja, S., Hornak, V., Yan, E. C., Syrett, N., Goncalves, J. A., Hirshfeld, A., Ziliox, M., Sakmar, T. P., Sheves, M., Reeves, P. J., Smith, S. O., and Eilers, M. (2009) Helix movement is coupled to

displacement of the second extracellular loop in rhodopsin activation. *Nat. Struct. Mol. Biol. 16*, 168–175.
45. Bokoch, M. P., Zou, Y., Rasmussen, S. G., Liu, C. W., Nygaard, R., Rosenbaum, D. M., Fung, J. J., Choi, H. J., Thian, F. S., Kobilka, T. S., Puglisi, J. D., Weis, W. I., Pardo, L., Prosser, R. S., Mueller, L., and Kobilka, B. K. (2010) Ligand-specific regulation of the extracellular surface of a G-protein-coupled receptor. *Nature 463*, 108–112.
46. Akal-Strader, A., Khare, S., Xu, D., Naider, F., and Becker, J. M. (2002) Residues in the first extracellular loop of a G protein-coupled receptor play a role in signal transduction. *J. Biol. Chem. 277*, 30581–30590.